University of Žilina
Faculty of Civil Engineering
Department of Building Structures and Bridges

Expert Assessment of the Static Recalculation of the Bridge "SO-20-20-05 Railway Bridge at km 3.706 – Pod Vyšehradem"

Prepared by: **prof. Ing. Josef Vičan, CSc.**
Ing. Jaroslav Odrobiňák, PhD.
Ing. Jozef Gocál, PhD.

Žilina 08/2018

TABLE OF CONTENTS

1. INTRODUCTION

The client SŽDC, státní organizace, Stavební správa západ with its registered office at Sokolovská 278/1955, 190 00 Praha 9 asked the contractor Žilina University, Faculty of Civil Engineering, by order No. 18/618 0001345, to prepare an expert assessment of the static recalculation of the bridge "SO-20-20-05 Railway Bridge at km 3.706 – Pod Vyšehradem" within the construction "Reconstruction of Railway Bridges Pod Vyšehradem" (Construction 2), section within the Reconstruction of the line Praha hl. n. (excl.) – Praha-Smíchov (incl.).

2. MATERIALS USED

The following documents were used to prepare the expert assessment:

[1] 2E_1_4_001: Technical Report – Bridge Structures. Reconstruction of Railway Bridges under Vyšehrad (Construction 2), section within the Reconstruction of the Line Praha hl. n. (excl.) – Praha-Smíchov (incl.). Construction part: Bridges, culverts and walls. Author: Association SP+MTP+SPEU_ Praha hl. – Praha-Smíchov. Responsible structure designer: Ing. Martin Vlasák, SUDOP Praha, a.s., bridge centre.

[2] 2E_1_4_003_1: SO-20-20-05 Railway Bridge at km 3.706 – Pod Vyšehradem. Existing condition – Ground plan and longitudinal profile. Reconstruction of railway bridges under Vyšehrad (Construction 2), section within the Reconstruction of the Line Praha hl. n. (excl.) – Praha-Smíchov (incl.). Construction part: Bridges, culverts and walls. Author: Association SP+MTP+SPEU_ Praha hl. – Praha-Smíchov. Responsible structure designer: Ing. Martin Vlasák, SUDOP Praha, a.s., bridge centre.

[3] 2E_1_4_003_2: SO-20-20-05 Railway Bridge at km 3.706 – Pod Vyšehradem. Existing condition – cross sections. Reconstruction of Railway Bridges under Vyšehrad (Construction 2), section within the Reconstruction of the Line Praha hl. n. (excl.) – Praha-Smíchov (incl.). Construction part: Bridges, culverts and walls. Author: Association SP+MTP+SPEU_ Praha hl. – Praha-Smíchov. Responsible structure designer: Ing. Martin Vlasák, SUDOP Praha, a.s., bridge centre.

[4] 2E_1_4_012_2: SO-20-20-05 Railway Bridge at km 3.706 – Pod Vyšehradem. Static recalculation of the load-bearing structure. Reconstruction of railway bridges under Vyšehrad (Construction 2), section within the Reconstruction of the Line Praha hl. n. (excl.) – Praha-Smíchov (incl.). Construction part: Bridges, culverts and walls. Author: Association SP+MTP+SPEU_ Praha hl. – Praha-Smíchov. Responsible structure designer: Ing. Martin Vlasák, SUDOP Praha, a.s., bridge centre.

[5] 2E_1_4_012_2_1: SO-20-20-05 Railway Bridge at km 3.706 – Under Vyšehrad. Static recalculation of the load-bearing structure – Annexes. Reconstruction of railway bridges under Vyšehrad (Construction 2), section within the Reconstruction of the Line Praha hl. n. (excl.) – Praha-Smíchov (incl.). Construction part: Bridges, culverts and walls. Author: Association SP+MTP+SPEU_ Praha hl. – Praha-Smíchov. Responsible structure designer: Ing. Martin Vlasák, SUDOP Praha, a.s., bridge centre.

[6] 2E_1_4_012_3: SO-20-20-05 Railway Bridge at km 3.706 – Pod Vyšehradem. Recalculation of the substructure. Reconstruction of railway bridges under Vyšehrad (Construction 2), section within the Reconstruction of the Line Praha hl. n. (excl.) – Praha-Smíchov (incl.). Construction part: Bridges, culverts and walls. Author: Association SP+MTP+SPEU_ Praha hl. - Praha-Smíchov. Responsible structure designer: Ing. Martin Vlasák, SUDOP Praha, a.s., bridge centre.

[7] 2E_1_4_011_3: SO-20-20-05 Railway Bridge at km 3.706 – Pod Vyšehradem. Detailed inspection of the steel NK. Reconstruction of railway bridges under Vyšehrad (Construction 2), section within the Reconstruction of the Line Praha hl. n. (excl.) – Praha-Smíchov (incl.). Construction part: Bridges, culverts and walls. Author: Association SP+MTP+SPEU_ Praha hl. – Praha-Smíchov. Responsible structure designer: Ing. Martin Vlasák, SUDOP Praha, a.s., bridge centre.

[8] 2E_1_4_011_3_1: SO-20-20-05 Railway Bridge at km 3.706 – Under Vyšehrad. Detailed inspection of the steel NK – Annexes. Reconstruction of railway bridges under Vyšehrad (Construction 2), section within the Reconstruction of the Line Praha hl. n. (excl.) – Praha-Smíchov (incl.). Construction part: Bridges, culverts and walls. Author: Association SP+MTP+SPEU_ Praha hl. – Praha-Smíchov. Responsible structure designer: Ing. Martin Vlasák, SUDOP Praha, a.s., bridge centre.

[9] 2E_1_4_011_4: SO-20-20-05 Railway Bridge at km 3.706 – Pod Vyšehradem. Detailed inspection of the substructure. Reconstruction of Railway Bridges under Vyšehrad (Construction 2), section within the Reconstruction of the Line Praha hl. n. (excl.) – Praha-Smíchov (incl.). Construction part: Bridges, culverts and walls. Author: Association SP+MTP+SPEU_ Praha hl. – Praha-Smíchov. Responsible structure designer: Ing. Martin Vlasák, SUDOP Praha, a.s., bridge centre.

[10] 2E_1_4_011_4_1: SO-20-20-05 Railway Bridge at km 3.706 – Under Vyšehrad. Detailed inspection of the substructure – Annexes. Reconstruction of railway bridges under Vyšehrad (Construction 2), section within the Reconstruction of the Line Praha hl. n. (excl.) – Praha-Smíchov (incl.). Construction part: Bridges, culverts and walls. Author: Association SP+MTP+SPEU_ Praha hl. – Praha-Smíchov. Responsible structure designer: Ing. Martin Vlasák, SUDOP Praha, a.s., bridge centre.

[11] 2E_1_4_011_2: SO-20-20-05 Railway Bridge at km 3.706 – Under Vyšehrad. Static and dynamic load test. Reconstruction of railway bridges under Vyšehrad (Construction 2), section within the Reconstruction of the Line Praha hl. n. (excl.) - Praha-Smíchov (incl.). Construction part: Bridges, culverts and walls. Author: Association SP+MTP+SPEU_ Praha hl. – Praha-Smíchov. Responsible structure designer: Ing. Martin Vlasák, SUDOP Praha, a.s., bridge centre. Author: CTU Prague Faculty of Civil Engineering, Department of Steel and Timber Structures. Thákurova 7, 166 29 Prague 6. Responsible researcher: doc. Ing. Pavel Ryjáček, Ph.D.

[12] 2E_1_4_011_1: SO-20-20-05 Railway Bridge at km 3.706 – Pod Vyšehradem. Material testing of steels. Reconstruction of railway bridges under Vyšehrad (Construction 2), section within the Reconstruction of the Line Praha hl. n. (excl.) – Praha-Smíchov (incl.). Construction part: Bridges, culverts and walls. Author: Association SP+MTP+SPEU_ Praha hl. – Praha-Smíchov. Responsible structure designer: Ing. Martin Vlasák, SUDOP Praha, a.s., bridge centre. Author: CZ FERMET, Laboratories CZ FERMET, Buštěhradská 283, 272 03 Kladno.

[13] 2E_1_4_008_2: SO-20-20-05 Railway Bridge at km 3.706 – Under Vyšehrad. Steel statement SO-20-20-05. Reconstruction of railway bridges under Vyšehrad (Construction 2), section within the Reconstruction of the Line Praha hl. n. (excl.) – Praha-Smíchov (incl.). Construction part: Bridges, culverts and walls. Author: Association SP+MTP+SPEU_ Praha hl. – Praha-Smíchov. Responsible structure designer: Ing. Martin Vlasák, SUDOP Praha, a.s., bridge centre.

[14] ČSN EN 1990, Eurocode: Basis of structural design. Office for Standards, Metrology and Testing, 2011 (including relevant NA).

[15] ČSN EN 1991-1-1 Eurocode 1: Actions on Structures Part 1-1: General actions – Densities, self-weight, imposed loads for buildings, Czech Standards Institute, 03/2004 (including relevant NA).

[16] ČSN EN 1991-1-4, Eurocode 1: Actions on Structures Part 1-4: General actions – Wind loads. Office for Standards, Metrology and Testing, 4/2013 (including relevant NA).

[17] ČSN EN 1991-1-5, Eurocode 1: Actions on Structures Part 1-5: General actions – Thermal actions. Czech Standards Institute, 2005 (including relevant NA).

[18] ČSN EN 1991-2 Eurocode 1: Actions on Structures – Part 2: Traffic loads on bridges Czech Standards Institute 07/2005 (including relevant NA).

[19] ČSN EN 1993-1-1, Eurocode 3: Design of steel structures – Part 1-1: General rules and rules for buildings. Office for Standards, Metrology and Testing, 12/2006 (including relevant NA).

[20] ČSN EN 1993-1-5 Design of steel structures – Part 1-5: Plated structural elements. Czech Standards Institute 02/2008 (including relevant NA).

[21] ČSN EN 1993-1-8 Eurocode 3: Design of steel structures. Part 1-8: Design of joints. Office for Standards, Metrology and Testing, 07/2011 (including relevant NA).

[22] ČSN EN 1993-1-9 Eurocode 3: Design of steel structures. Part 1-9: Fatigue. Office for Standards, Metrology and Testing, 12/2013 (including relevant NA). [23] ČSN EN 1993-2, Eurocode 3: Design of steel structures – Part 2: Steel bridges. Czech Standards Institute 01/2008 (including relevant NA).

[24] Statický přepočet ocelové nosné konstrukce příhradového mostu přes Vltavu v km 3, 706 trati Praha hl. nádraží – Praha Smíchov. TOPCON servis s.r.o., 2004.

[25] Metodický pokyn pro určování zatížitelnosti železničních mostních objektů. SZCZ 09/2015.

[26] Závěrečná zpráva projektu COST CZ - LD15127 - Pokročilé metody posuzování degradovaných ocelových konstrukcí, ČVUT v Praze, 2017.

[27] GARCÍA M. O. The Impact of the Connection Stiffness on the Behaviour of a Historical Steel Railway Bridge. Thesis. Faculty of Civil Engineering, CTU in Prague, 2017.

3. DESCRIPTION OF THE BUILDING

3.1 Building Identification Data

Name of the construction:	Reconstruction of Railway Bridges under Vyšehrad (Construction 2), section within the Reconstruction of the Line Praha hl. n. (excl.) – Praha-Smíchov (incl.)
Level of documentation:	Preparatory documentation (PD) and project proposal (PP)
Characteristics of the construction:	Linear railway construction, modernisation of the railway line
ISPROFIN number:	511 352 0019
Client's CfW number:	E618-S-12006/2016/Šim
Contractor's CfW number:	16 354 201
Place of construction:	Railway line 0201 Praha hl. n. – Praha-Smíchov

	both lines are part of the national railway of European importance (E)
Region:	Capital City of Prague
Municipality / Municipal district:	Prague 2, Prague 5
Cadastral territory:	cadastral territory of Vyšehrad, cadastral territory of Smíchov
Designated municipal authorities:	Prague 2, Prague 5
Municipalities with extended powers:	Capital City of Prague
Client:	Správa železniční dopravní cesty, státní organizace with registered office: Prague 1003/7, 110 00, Nové Město, Dlážděná 1/7, 110 00
Organisational component:	Stavební správa západ, Sokolovská 278/1955, 190 00 Prague 9
For the investor:	Ing. Petr Vaníček, SŽDC, s.o., Stavební správa západ
Author:	"SP+MTP+SPEU_Praha hl. – Prague-Smíchov" established by the Company Agreement dated 04/08/2016 Partners of the Company Company name: SUDOP PRAHA a.s. Registered Office: Prague 3, Žižkov, Olšanská 2643/1a, 130 00 ID No.: 25793349, VAT No.: CZ25793349 and Company name: METROPROJEKT a.s. and Company name: SUDOP EU a.s.
Chief Project Engineer:	Ing. Michal Mečl AI in the field of transport construction No. 0009519
Chief Project Engineer (Construction 2):	Ing. Tomáš Martinek, SUDOP PRAHA, a.s.
Responsible designer of the structure:	Ing. Martin Vlasák, SUDOP PRAHA, a.s., AI in the field of Bridges and IK and in the field of Transport Construction No. 0009271
Cooperation:	Ing. Jaroslav Voříšek, SUDOP PRAHA, a.s.

3.2 Identification Data of the Structure

Name of the structure:	SO 20-20-05 Pod Vyšehradem Bridges, railway bridge at km 20-20-05 – Pod Vyšehradem
Common name:	Pod Vyšehradem
Track section:	Line section 0201 Praha hl. n. (excl.) - Praha-Smíchov (incl.)
Definitional section: (station section)	DÚ 04 Praha-Vyšehrad – Praha-Smíchov
Type of load-bearing structure:	steel riveted parabolic truss with lower element rail-track common for both converted tracks
Description of the substructure including wings	
stone abutments,	stone piers
surface foundation (P02 and P03 on caisson)	on wooden piles (O02) stone wings parallel and perpendicular at O02
Number of bridge openings:	3
Number of tracks:	2
Length of bridging:	215.550 m
Bridge length:	234.450 m
Span of the load-bearing structure:	71.72 m under track Nos. 1 and 2
Construction height:	1.380 m (to LT) under track Nos. 1 and 2
Decisive height of the railway bed contour	flat-laid bridge deck (vertical bolt) (structure without rail bed)
Free height under the bridge.	3.74 m (right bank pavement)
Perpendicular hole clearance:	7.73 m (Vltava – max Q plav =188.28 m a.s.l. Bpv)
Hole 1.	69.045 m
Hole 2:	69.145 m
Hole 3:	69.450 m
Bridge inclination (right/left, angle of inclination):	90°
Angle of crossing with a bridged obstacle:	approx. 80°
Bridge width:	13.580 m (including footbridge brackets)
Clear width on the bridge:	8.108 (between portal perpendiculars)
Year of construction (production) of the NK:	1901 (RZ 1901)
	O01: 1901 (RZ 1901) P01: 1901 (RZ 1901) P02: 1901 (RZ 1901) O02: 1871 (modifications 1901)
Year of last reconstruction or repair of the structure:	1987 repair (MES) 1957 paint restoration (MES) 1912 repair of the substructure (MES)
Load data to date:	z_{UIC} = 0.41 (supporting cross bar connection to main beam)

Construction condition of the load-bearing structure	Grade 3 substructure – level 2
Bridge equipment:	external footbridge brackets
River km:	Vltava river km 55.35
Load on the bridge:	axle load category **C3/60** (see TTP)

The day beacons, including lighting, are managed and owned by Povodí Vltavy s.p.

Important note: cultural immovable monument since 2004, CLCM reg. no. 101 315.

3.3 Description of the Bridge Structure

The railway bridge at km 3.706 bridges the Vltava River with three bridge openings. The load-bearing structures were made in 1901 from mild steel. They are designed as closed truss multiple systems with a curved upper chord with the same span of 71.72 m in all bridge openings. The structural arrangement of the bridge corresponded to the time of its construction and the effort to reduce the weight of the structure. The individual sections are graded according to the expected stresses. The details of the truss segmented rods were not designed with regard to the risk of steel corrosion in case of failure of the corrosion protection (especially crevice). This problem particularly affects the lower chord and lacings.

The bridge is double-lined with a lower elemental rail-track, consisting of supporting cross bars and unconnected longitudinal trusses inserted between the supporting cross bars. The axial distance of the main beams is 8.80 m. The height of the main beam varies from 7.136 m at the portal to 12.347 m in the centre of the span. The shape of the upper chord is polygonally broken in the place of the centres. The main beam is divided into 16 trusses with lengths of 3.46 m + 4.0 m + 4.40 m and 5 x 4.80 m at mid-span.

The upper chord consists of a double-walled Π-shaped section with a clearance of 416 mm. The wall has a constant height of 470 mm throughout the length of the chord and a constant thickness of 24 mm, which consists of two plates of 12 mm each. The progression of the increasing axial force is taken into account by changing the thickness of the top chord, which is graded from a basic thickness of t_1 = 10 mm in the first chord by 10 mm up to a thickness of 70 mm in the middle of the span. The connection of the chord to the walls is made with 4 angles 110 x 110 x 14 mm and rivets ∅ 22 in the walls or ∅ 24 in the chord. The shape of the cross-section of the rods of the upper chord is ensured by plate beam diaphragms riveted to the walls and chords in thirds of the span of the trusses. The lower chord of the main beam has a double-walled open section of 416 mm with a constant wall height of 560 mm and a thickness of 24 mm. The change in axial forces is taken into account by grading the lower chords up to a thickness of 57 mm and a width of 410 mm. The connection between the walls and the chords is again made using 4 angles 110 x 110 x 14 mm and rivets ∅ 22 in the walls or ∅ 24 in the chords. The shape of the cross-section is again ensured by plate beam diaphragms riveted to the walls at the mid-span of the trusses and in the panel points.

The lacings D_1 to D_3 have a segmented cross section consisting of 2 quadrants of 80 x 80 x 9 angles, each reinforced by a pair of chords ▭ 360 x 14 mm (D_1), ▭ 400 x 14 (D_2) and ▭ 340 x 12 (D_3). Lacing D_4 consists of 2 quadrants of angles 80 x 80 x 8 reinforced again by a pair of chords ▭ 320 x 10 mm. Lacings D_5 to D_7 are made of only 2 quadrants of angles 90 x 130 x 12 (D_5), 80 x 120 x 11 (D_6) a 80 x 100 x 10 (D_7) without chords. The cross-section of the lacings D_8, D_9 and D_{10} is made of only pairs of angles 80 x 100 x 13 (D_8), 90 x 90 x 10 (D_9) and 80 x 80 x 8 (D_{10}). The connection of quadrants and pairs of angles into a segmented cross-section is ensured by truss connectors ▭ 60 x 8 mm. The connection to both chords is made by riveted joints with rivets ∅ 22 mm.

The perpendiculars of the main beam, except for the extreme portal perpendicular, also have a segmented cross-section. The cross-sections of perpendicularsV_1 to V_3 consist of 2 quadrants of angles 100 x 150 x 14 (V_1), 90 x 130 x 14 (V_2) and 90 x 130 x 11 (V_3) connected into a segmented cross-section with truss connectors ▭ 60 x 13 mm. The perpendiculars V_4 to V_8 have a segmented cross-section consisting of 2 pairs of angles 100 x 150 x 14 (V_4), 90 x 130 x 14 (V_5), 80 x 120 x 12 (V_6), 80 x 100 x 12 (V_7) a 80 x 80 x 10 (V_8), which are connected by truss connectors ▭ 60 x 13 mm. The connection of the perpendiculars with both chords is made with rivets ∅ 20 mm. The cross-section of the end portal perpendicular consists of 16 angles 100 x 100 x 12 folded into section I. The chords, consisting of 8 angles and 2 x 12 x 600 mm infill plates, are connected along the entire height of the perpendicular with 13 mm thick plates.

The lower elemental rail-track is composed of longitudinal trusses and supporting cross bars. The longitudinal trusses have a differentiated cross section with respect to the different bays. The longitudinal section in bay 0 – 1 consists of a wall ▭ 690 x 10 mm connected by 4 angles 80 x 80 x 10 with chords 190 x 10 (lower) and 250 x 10 (upper). Connection securing neck and chord rivets Ø 20 mm with 120 mm spacing. The longitudinal truss in bay 1 – 2 has the same wall and chords, but their connection is ensured by angles 80 x 80 x 10 with neck and chord rivets Ø 20 mm with spacing of 120 mm. Similarly, the longitudinal truss in bay 2 – 3 is designed in a similar way, so that the cross section differs only by the 90 x 90 x 10 angles. The longitudinal trusses in the other bays have ▭ 220 x 10 (bottom) and ▭ 280 x 10 (top) section chords connected to the ▭ 690 x 10 mm wall by 100 x 100 x 12 mm angles and Ø 20 mm rivets at 120 mm intervals.

The supporting cross bars also have a differentiated cross-section. Supporting cross bar 0 (outermost) consists of a ▭ 1 030 x 13 mm wall connected to ▭ 400 x 20 mm chords by 110 x 110 x 13 mm angles. The neck rivets have a section of 22 mm and their spacing is 100 mm. This cross-section has a transom in the central part and under the inner longitudinal trusses. The cross-section of the chords is graded to a section of 400 x 10 mm in the outermost parts. The cross-section of supporting cross bar 1 and 2 differs only in the thickness of the chords, which is 400 x 26 mm in the central part, in the outermost parts it transitions into a cross-section ▭ of 400 x 14 mm. Supporting cross bars 3 to 8 have the same cross-section consisting of a wall ▭ 1 030 x 13 mm connected to the chords ▭ 400 x 30 mm by 4 angles 110 x 110 x 13.
The chords are 2 x graded to a ▭ 400 x 20 mm section under the outer longitudinal truss and ▭ 400 x 10 mm in the sections adjacent to the main beams. The neck rivets of the crossbars are generally Ø 22 with spacing of 100 mm. The mounting joints of all crossbars consist of 27 rivets Ø 22 mm arranged in 3 rows of 9 rivets. The connection of the crossbars to the main beams is again riveted with Ø 20 mm rivets.

The connection of the longitudinal trusses to the supporting cross bars is the same for all longitudinal trusses. It is solved by connecting only the walls of both elements using 2 x L 80 x 80 x 8 angles on both sides of the walls of the supporting cross bars. The number of rivets in the longitudinal wall is 7, while the outermost rivets have a section Ø 20 mm, the inner rivets have a section ∅ 22 mm.
The joint is completed by 18 rivets in the supporting cross bar wall Ø 22 mm.

As part of the reconstruction of the bridge in 1987, the longitudinal trusses were supplemented with rail-track stiffening and a brake stiffener. The perimeter sections of the brake stiffener are made of a pair of angles 125 x 125 x12 mm. The inner lacings are made of 125 x 125 x 12 mm angles in the part between the longitudinal bars or 90 x 90 x 12 mm angles in the central part. The height of the brake stiffener truss is 1,700 mm in the 2nd truss and 2 x 1,600 mm in the 8th and 9th truss.

The longitudinal stiffening of the bridge under the rail-track is a composite system consisting of a solid section riveted from 2 L 110 x 110 x 12 mm in the first 4 trusses. The lacings in bay 5 are of cross-section 2 L 100 x 100 x 12 mm, in bay 6 2 L 100 x 100 x 10 mm,

in bay 7 2 L 90 x 90 x 10 and in bay 8 2 L 80 x 80 x 10 mm. The upper stiffening over the rail-track was reconstructed in 1987 and replaced with a new one. It consists of a rhombic system with partitions made of welded sections P14 x 600 + P 20 x 2 300 in the portal, or P12 x 300 + P12 x 200 + P14 x 180 in the other interfaces and lacings composed of two 90 x 90 x 8 mm angles in a double-sided section.

The reconstruction in 1987 included also the outermost portals. The portal mullion is made of symmetrical welded I section with P14 x 600 mm plate wall and P20 x 300 mm chords.

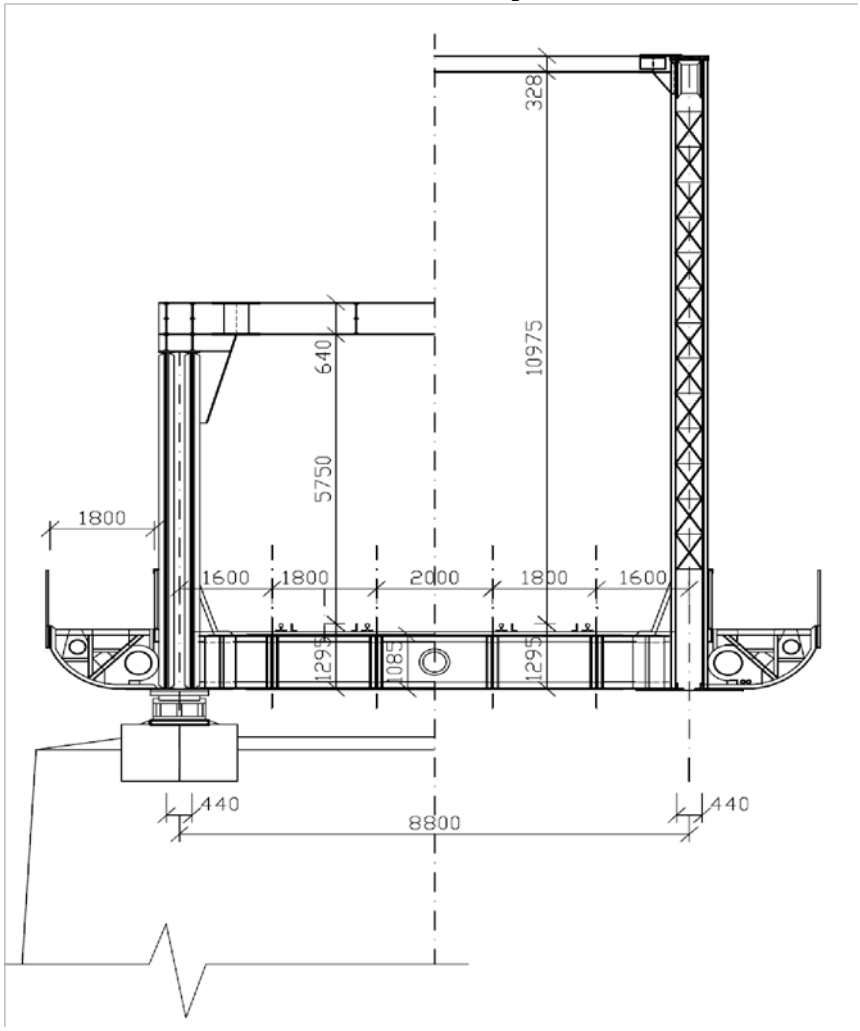

Fig. 3.1 Layout cross-section through the load-bearing structure

Pedestrian bridge cantilevers are attached to both main beams with a clear width between the railings of 1,820 mm. The brackets are connected via the splice plate to the section of the perpendiculars and then to the lower chord of the lower flange. In the longitudinal direction, the brackets are connected on the outside by a continuous U-shaped ledge beam consisting of a P7 x 450 mm wall and chords from L 70 x 70 x 7 mm angles. On the inner side there is a longitudinal truss of U-section of 260 mm height. The outer ledge longitudinal truss and the inner longitudinal truss are connected to each other in the middle of the trusses by an intermediate supporting cross bar. The height of the railing on both sides of the footbridge is approximately 1,130 mm above the walking surface, which is made of 50 mm thick wooden beams.

The load-bearing structures are supported on steel bearings. The dilatation movement of all constructions is from Smíchov towards Vyšehrad. The moving bearings are cylindrical roller bearings with five Ø 160 mm rollers and a bascule. Fixed bearings are rack mounted.

The weight of one load-bearing structure, including its bridge equipment, was found to be 593 t from the steel statements in the archive documentation.

The substructure is solid of coursed rubble, with concrete infill. Piers P01 and P02 have stone storage thresholds which transition into stone shafts with variable widths of 3.15 m to 4.18 m and variable lengths of 13.95 m to 14.98 m. The variability in shape is provided by the faces of the shaft sloping approximately 1:20 from the perpendicular. The stone shafts are placed on stone foundations 5.20 m wide, which were built on steel riveted caissons. The interior of the caissons was filled with plain concrete after the foundation work was completed.

The stone abutment O02 from 1871 consists of an abutment, parallel wings and separate perpendicular wings. The common base of the support and parallel wings is based on a wooden grid and wooden piles. The abutment with a shaft width of approx. 13.73 m and thickness of approx. 4.00 m is intended for the placement of the load-bearing structure from bay 3, including the connection of the bilateral load-bearing structure footbridges to the final abutment wall. The abutment is connected to the stone parallel wings, which between them hold the body of the double-track railway line crossing the adjacent embankment. The walkways emerging from the footbridges descend along the parallel wings, the slopes of the earthwork outside the parallel wings are intercepted by stone perpendicular wings. Abutment O01 is a common support of the load-bearing structure of the structure SO 20-20-05 and the structure SO 20-20-04.

4. EXPERT ASSESSMENT

4.1 General In addition to the static recalculation of the bridge at km 3, 706 – Pod Vyšehradem, we focused on other annexes specified in more detail in Chapter 2, which are directly and indirectly related to the static recalculation. The purpose and objective of the subject static recalculation was to determine the load capacity and to assess the compatibility of the existing bridge structure, especially the supporting steel structures constructed in 1901, taking into account their current construction condition. At the same time, the static recalculation was the basis for the design of the bridge reconstruction, which is conceived with the assumption of using the existing load-bearing structures with the possibility of prolonging the operation for the next 30 years while maintaining at least the current compatibility of the C3/60 (TTZ C3/60) axle load category, which, however, will allow a prospective increase in the number of train capacities almost twofold. The recalculation of the existing bridge structure was carried out in category D according to MP 2015 [25], which respects the sets of valid standards ČSN EN 1990 – ČSN EN 1996.

The authors of the static recalculation have proceeded very responsibly in its preparation, as evidenced by the addition of additional documents necessary for the consistent execution of the static recalculation and the statement of real conclusions and results of the recalculation. Therefore, the following documents were secured for a responsible recalculation:

a) verification of the dimensions of the steel structures and the substructure (global measurement, local cross-sectional measurement),
b) preparation of drawings (existing condition) of the supporting load-bearing steel structures and their substructure,
c) detailed inspection of the bridge's steel load-bearing structures with determination of corrosion losses of OK elements,
d) testing of steel samples (mechanical tests, metallographic tests, analysis of chemical composition),
e) detailed inspection of the stonework of the abutments and piers (underwater and overwater parts),
f) performing static and dynamic verification load tests to verify the real behaviour of the bridge structure,

g) determination of stress spectra for fatigue failure limit state assessment,
h) analysis of the history of traffic load on the line.

The result of the static recalculation showed that the load-bearing structures of the bridge structure are limiting in terms of its load-bearing capacity and therefore also the compatibility of the TTZ C3/60 operational load. The stone substructure does not exhibit any significant static failures and was therefore not limiting in terms of the load capacity of the existing bridge structure. The abutments show the consequences of the lack of function of the movable bearings due to their corrosion, which prevented free rotation, which was manifested by the displacement of the upper row of stone blocks. These parts of the abutment were rehabilitated with steel bolts probably in 1987 as part of the reconstruction of the rail-track. However, the damage has now moved down a row below the bolts where the damaged masonry was regularly jointed. The determination of the load capacity of the substructure of the bridge (piers P01, P02 and abutments O02) was therefore carried out according to the new principles given in [25] in category C. However, its determination assumed the repair of the identified defects and the reinforcement of the gapped inner part of the masonry by grouting.

4.2 Analysis of the Static Recalculation of the Load-Bearing Structures of the Bridge at km 3.706 – Pod Vyšehradem

4.2.1 Material Tests

The authors of the static recalculation followed the procedure in Article A. 1.1.1 (b) of [25] and carried out material tests. These included mechanical tests to determine the strength characteristics of the steels used in the existing bridge load-bearing structures, hardness tests to verify the quality of the material, as well as analysis of the chemical composition of the steels and metallographic analysis. The results of the conducted tests confirmed that it is a mild steel with strength characteristics very close to those given by [25] for the purpose of static calculations. According to the conclusions in [4], the results of the mechanical tests indicate a higher yield strength value than that given in [25], whereas the results of the hardness tests indicate a higher breaking strength.

Conclusion:

The results of the material tests were not statistically evaluated in the sense of Article 4.4.8 in [25], or statistical evaluation was not provided to the authors of this assessment. However, the conclusions drawn from the test results can be accepted.

Similarly, the conclusions of the analysis of the Charpy impact tests, which showed properties in terms of the value of impact work close to the quality of JR grade steels, are correct and correctly point to the unsuitability of the application of this steel for dynamically stressed structures.

Note: The characteristic value of the breaking strength of the mild steel given in Tab. A. 1 in [25] is 360 MPa. On page 17 in [4] the value fu = 340 MPa is incorrectly stated.

4.2.2 Detailed Inspection of the Load-Bearing Structures of the Bridge

A detailed inspection of the steel load-bearing structures is an essential condition for the structural design of each bridge. It is also an important condition in terms of determining the reliability level introduced in [25] for verifying the reliability of existing bridge structures. Therefore, due attention was paid to the detailed inspection by the authors of the static recalculation. A description of the implementation of the detailed inspection is given in [7] and [8]. The detailed inspection, in addition to verifying the geometric parameters of the load-bearing structures and refining the specification of the permanent load on the bridge structure,

focused mainly on the corrosion damage of the steel structures. The corrosion weakening of the steel structure elements was documented by means of so-called element cards, where the structure is divided into groups of elements with their unambiguous designation. To identify the position of the defect, the local stationing of the element is also used, which is relative to the length of the element from 0 at the beginning to 1 at the end of the element. Within an element, defects are identified by a serial number. An unambiguous code designation is used to describe the defect. The photo documentation taken has the same code designation, which allows the defects to be monitored during subsequent inspections.

As a result of the detailed inspection, the corrosion weakening of the individual elements was determined and used in the modelling of the steel structure and for the design of its elements and cross-sections. The analysis of the results of corrosion attack on the steel structures of the bridge led to significant conclusions in terms of durability and further exploitation of the bridge.

The segmented infill rods composed of angles provide very favourable conditions for crevice corrosion. This type of corrosion is most pronounced in the lacings and also in the perpendiculars of load-bearing structures. This is mainly the detail at the connection of the truss connector of the split rod between the pair of neck angles and the connection of the rods to the splice plates or directly to the bottom chord. As the authors of the static recalculation correctly state, this defect is very complicated to repair and they correctly propose the replacement of the affected elements.

The lower parts of the perpendiculars are significantly affected by corrosion at the connection to the splice plates of the lower chords. Then the completely corroded chords of the angles of these rods in the places of connection to the lower chords are serious. The cross-sections of the lower chords are structurally inappropriate and represent another element with more significant corrosion weakening. These are in particular the neck angles of the lower chords and the splice plates of the lower stiffening under the rail-track, including the above-bearing splice plates. The relatively wide lower chords of these cross-sections prevent both the ventilation of the cross-section and the natural percolation of dirt and abrasion that accumulates inside the lower chords. The situation is worse especially for rods U4 to U8, where more significant corrosion losses of the internal chords of the neck angles can be observed. The failure can only be repaired by replacing these angles and splice plates.

The rail-track elements do not show as significant corrosion attack as the elements of the main beams. The longitudinal trusses are in relatively good condition in terms of corrosion. Local corrosion is only visible under the bridge beams, which, due to the sufficient load-bearing capacity of the longitudinal trusses, does not affect their load-bearing capacity significantly at present. The more significant problem with longitudinal trusses is cracks. The detailed inspection diagnosed 2 new cracks of 185 mm and 580 mm in the upper chords of the longitudinal trusses, which were not found in the structure during the detailed inspection in 2014. The supporting cross bars of the lower rail-track show pitting corrosion of the upper chords caused by bird droppings and moisture. At the point of connection of the brake stiffeners to the supporting cross bars, corrosion of the crossbar wall occurs, again due to the effect of bird droppings and moisture, as the splice plates of the stiffening under rail-track and brake stiffening create favourable conditions for bird nesting.

From the above description of the shortcomings of steel load-bearing structures, it is possible to conclude the classic defects and failures that are the result of inappropriate structural design of the cross-sections of the rods of the truss bridges.

Conclusion:

The results of the detailed inspection and the conclusions of the recalculation authors in assessing the defects and faults found are correct. However, it is not clear from the technical report for the structural recalculation which failures have been implemented in the calculation model of the bridge load-bearing structures and which have not been taken into account, as they are assumed to be removed by maintenance or repair as required by Article 4.1.2 in [25]. Also the method of incorporation of the detected defects and failures, especially corrosion losses, into the calculation model of the structure is not described in detail.

4.2.3 Reliability Level of the Existing Structure

The reliability level of the existing steel structure was taken from [25]. To determine the load capacity, a reliability level for a residual life of 30 years was selected and based on this, the values of the partial reliability coefficients of the load effects and resistances of the cross-sections and elements of the steel bridge load-bearing structure were determined. For the assessment of the compatibility of the operational load of the TTZ C3/60, the coefficients for a residual life of 30 years were also used and in case of unsatisfactory transience they were subsequently reduced for a residual life of 5 years. The values of the partial reliability coefficients of the load effects and resistances of the cross-sections and elements of the steel structure were determined for the above residual lifetimes and were used in the determination of the design values of the load effects and resistances of the cross-sections and elements of the load-bearing structures of the subject bridge. **Conclusion:**

The reliability level for determining the load capacity of the steel load-bearing structures of the bridge structure at km 3, 706 – Pod Vyšehradem was determined correctly.

Note: For the purpose of bridge structure recalculations, the values of the reliability index βt in Tab. F. 1 were determined from the design value βd = 3.65. This value corresponds to the design life of the new structure Td = 100 years. The value βd = 3.80 corresponds to a life of T = 50 years. In the Standard [14], the life for building structures is given as Td = 50 years, while for bridges it is Td = 100 years. Thus, the reliability index value for bridges given in the relevant standards is higher than it should be according to the specified life.

4.2.4 Load Analysis

The load capacity of the bridge load-bearing structures was determined according to MP 2015 [25], which is in accordance with the methodology of the ČSN EN set of standards. The considered load model of the moving load for the determination of the load capacity is LM 71 with a load classification factor α=1.00. The dynamic coefficients are considered by the values of Φ3(or Φ2 for fatigue) for a standard maintained track. The design load effects were determined using the relevant partial load factors defined in [25] for the respective design residual life of the bridge. The individual load states were assembled into partial envelope states called load state groups, which were further combined with each other. The load combinations were used from the standard [14]. In terms of combinations, the rail load was treated as a single multi-component load, i.e. groups gr11 and gr12 etc.

We have the following comments and observations on the load analysis:

a) The weight of the unmodelled elements is taken into account by increasing the bulk weight of all rods by a flat rate of 25% (page 31 in [4]). It would probably be more appropriate to consider different values for the rail-track elements and different values for the rods of the main beams, since the rail-track elements have a different nature of connection to each other and to the main beams. If this fact were to be taken into

account, it would probably result in a lower load capacity of the supporting cross bars, which are the limiting elements in terms of load capacity.

b) The considered wind load on the windward beam of 100% and on the outermost beam only 50% is contrary to the Standard [16]. While this simplification has a realistic basis, it should have been applied only up to the amount of traffic load. Thus, from a height of 4.0 m from the top of the rails it is necessary to load both main beams with the full wind load (see figure below). At the same time, according to [16], it is possible to consider the wind load on the rail-track only on the windward beam. The eccentricity of the action of the horizontal component of the wind load on the web of the moving load should be correctly considered from the plane of the rail-track stiffening. This also applies to side impact loading.

c) The eccentricity of the load model 71 in the transverse direction due to the non-uniformity of the wheel forces according to 6.3.5 of [18] has been taken into account correctly. However, it is not clear whether the actual position of the track on the bridge was considered, i.e. whether its position was determined by measurement.

d) For the assessment of the global load-bearing system, a pavement load of 1.9 m was considered along with the railway traffic on the bridge. A combined load value of 3.0 kN.m^{-2} is considered. This value is recommended in Standard [18] for pedestrian loads on road bridges, but since this Standard [18] does not specify a value for railway bridges, it can be accepted. The position of this load is also considered due to the ineffective position of the pedestrian loads for the infill rods, but the simplification is acceptable given its size.

Note: In the text and below the figures, the term accidental long-term load is used, which has already been dropped from our terminology in accordance with the terminology of the Eurocodes.

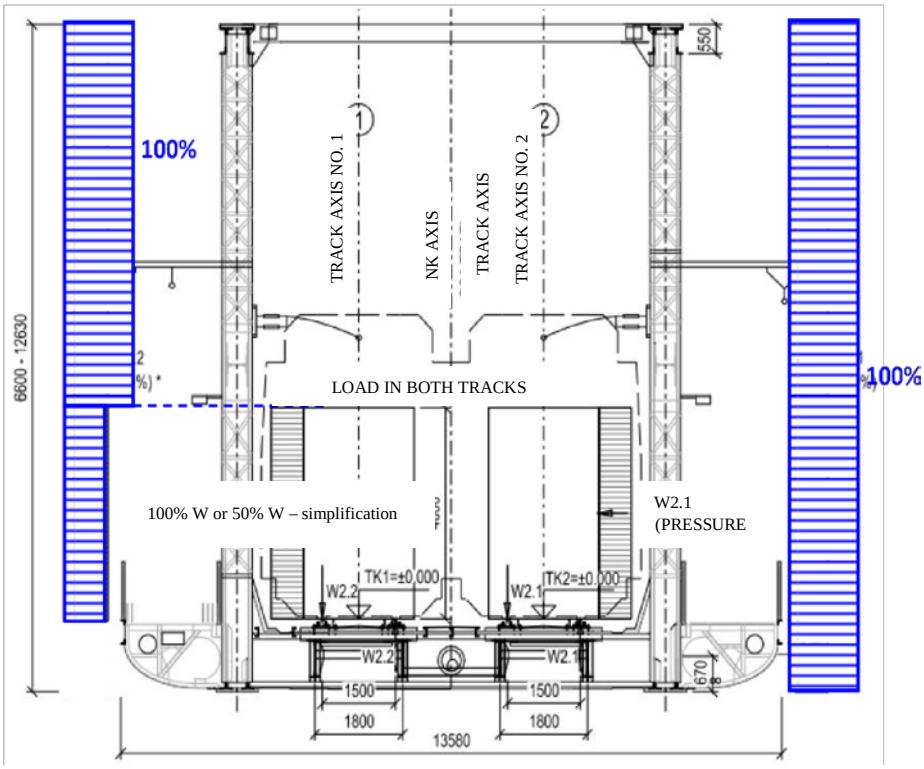

Fig. 4.1 Simplified application of wind loads to a steel load-bearing structure

Conclusion:

The loading of the bridge load-bearing structures in km 3, 706 – Pod Vyšehradem was determined correctly with respect to the relevant standards and MP 2015 [25]. Applied exceptions (wind loads on the structure, pedestrian loads) are realistic and acceptable.

The authors of the assessment make some comments, but these do not significantly affect the results of the static recalculation.

4.2.5 Traffic Load Survey on the Line

In order to assess the ultimate fatigue state, a detailed analysis of the traffic load on the bridge was carried out during the total lifetime of the bridge, i.e. from 1901 to 2055. For the period up to 2000, the analysis of the development of traffic intensity is based on the use of available historical documents, which have been used to estimate the total volume of traffic (in million gross tonnes) as well as the ratio between freight and passenger transport. For the ultimate fatigue state assessment itself, the relative stress spectra according to ČSN 73 6203:86 are used, which have been transformed for the loading scheme of the C3 axle load category and applied to the double line bridge.

For the evaluation of the current railway traffic on the bridge from 2001 to 2018, as well as for the assumption of traffic development in the period from 2018 to 2055, the current traffic composition is based on the SZCZ timetable, on the basis of which a total of 14 groups of characteristic trains were defined, of which 12 groups of passenger trains and 2 groups of freight trains. These groups were then used to determine the spectra of the oscillations by means of a dynamic analysis of their transitions, but this is not part of the documentation under consideration and the static recalculation only refers to the final report of the project [26], which dealt with it.

Conclusion:

The authors of the report state that the survey of the development of traffic load during the entire lifetime of the bridge (existing and planned future) was carried out very carefully and with maximum use of all available means. The result is a qualified estimation of the actual history of rail traffic loading, which is a basic prerequisite for subsequent reliable assessment of the ultimate fatigue state or for determination of the residual fatigue life of the bridge. In this context, the estimate of the future traffic load is questionable and appears to be significantly overestimated (see also 4.2.9).

4.2.6 Computational Model

To calculate the internal forces of the global structural system, a 3D rod calculation model was created in MIDAS Civil 2016. For the sake of clarity of the results and the capacity of the computational software, the basic model was divided into 3 partial models for:

a) global structural analysis of the structure (envelope of the moving load, total load combination),
b) global dynamic analysis of the structure (specific boundary conditions – eigenmodes and frequencies),
c) analysis of the structure (generated states from moving loads for stability combinations, imperfect model for calculation of the effect of second-order theory – non-linear calculation). The computational models are described in a clear and detailed manner in accordance with the requirements prescribed in [25]. In order to represent the real load distribution, bridge beam rods and rail rods were added to the calculation model of the structure. These rods are released by means of end ties so that they do not interact with the bridge load-bearing structure model. In connection with the refinement of the modelling of the real behaviour of the steel structure, semi-rigid panel points and semi-

rigid connections of rail-track elements were implemented in the calculation model. To determine the relative values of the stiffness parameters of the panel points and connections, the results of calculations performed in the IDEA StatiCa program (Connection module) within the project [26] and the master thesis [27] were used. We have the following comments on the modelling of semi-rigid panel points and nodes:

a) When using submodels, it is always a major problem to capture their boundary conditions to the extent that they correctly capture the realistic effect of the detail in the whole structure, or model of the whole structure. In the analyses from which the results were taken, only half of the panel points are even modelled, which makes it even more difficult to capture the correct action of the detail in the whole system.

b) In the case of the detail of the connection of the supporting cross bar to the main truss, the reduction of the bending stiffness in the horizontal direction is only 5 to 7% of the original stiffness, which in our opinion represents an underestimation of the actual stiffness of the connection of the lower chord of the supporting cross bar. As an example, consider the statement of the authors of the static recalculation one page further on in the analysis of the stiffness of the longitudinal trusses in paragraph 3.4.1.2, where it is stated that the ratio of the wall stiffness to the total stiffness of the section is about 5%. In the case of the supporting cross bar it is similar, however, its lower chord is anchored with one chord of the lower flange of the main beam and with the other chord of the lower flange of the main beam through the extension. The splice plate is additionally reinforced with a lower stiffening splice plate. Increasing the stiffness in the horizontal direction would have the effect of better redistribution of horizontal moments in the supporting cross bars.

c) Similarly, in the case of the connection of the longitudinal trusses to the supporting cross bar, its normal stiffness is considered to be a very small value, only 15%. The rationale of the static recalculation in paragraph 4.7.3 on page 131 includes the sentence that the normal stiffness of the wall connection corresponds to only 40% of the normal stiffness of the wall. However, it is not clear on what basis this claim is based. In our opinion, this simplification represents an underestimation of the true normal stiffness of the connections of the longitudinal trusses to the supporting cross bars, with the consequent reduction of the stresses on the longitudinal trusses by axial forces and on the supporting cross bars by horizontal bending moments from the interaction of the rail-track with the main beams.

d) An interesting simplification is reported by the static calculation authors when modelling segmented rods. It is a reduction of the bending stiffness to the immaterial axis of the cross-section of the rod to take into account its shear compliance. This model is basically applied in the calculation of the critical force of the rod in relation to its immaterial axis, but it takes into account the increase in deformation and thus the bending moments of the shear-resisting rod according to the second-order theory. However, it is questionable whether the values of 0.5 – 0.6 of the real moment of inertia to the immaterial axis of the rod were determined correctly, as they are very low. This reduction should be redistributed between the bending stiffness EI_z and the shear stiffness GA_y of the modelled rod so that the resulting deformation is the same. The introduction of a surrogate bending stiffness in the calculation model means an increased reduction of the bending moments determined by static linear analysis according to first-order theory. At the same time, this approach does not take into account another phenomenon of the segmented rod model, which is the interaction of global and local buckling of the rod.

Conclusion:

The choice of the computational model was correct on the part of the authors. The computational model is described in detail in accordance with the requirements of MP 2015 [25]. The authors of the static recalculation paid special attention to the modelling of the individual connections of the main beam rods and rail-track elements, as well as their mutual connections. Here, we have some reservations about the stiffness values of selected connections, particularly the supporting cross bars to main beam connections and the longitudinal trusses to supporting cross bars connections, which are analysed in the comments above. We consider it inappropriate to apply such significantly reduced bending stiffnesses of segmented rods to their immaterial axes in the calculation model of the whole structure. This approach leads to an overestimation of the influence of the shear compliance of the rod, on the other hand it does not take into account the interaction of the global and local brace of the rod.

4.2.7 Construction Analysis

4.2.7.1 Global Construction Analysis and Second-Order Theory Impact Analysis

A resilience global analysis was performed in accordance with MP 2015 [25] with following considerations:

- the global imperfections according to Article 5.3.2 (2) in Standard [23] for the design of the main load-bearing elements of the bridge by means of surrogate forces (see also Article 5.3.2 (7) and (8) in Standard [19]), which are used to express the global imperfections of the reinforcement system according to Article 5.3.3 (1) in Standard [23] with respect to the nature of the structure,
- without introducing the local imperfections of individual rods directly into the design model of the structure and by taking them into account according to Article 5.3.4 (1) in the Standard [23] by means of brace coefficients determined on the basis of the stability calculation for individual rods.

The stability analysis of the structure (LBA) showed that the influence of the second-order theory did not need to be considered, as the LBA resulted in a critical multiplier of α_{cr} = 13.55. However, the authors of the static recalculation have attempted to take into account the influence of the second-order theory with respect to the method of assessment of individual rods.

They applied the nonlinear calculation on an imperfect rod structure model (GNIA). They created an imperfect model by introducing the curvature of the upper chords of the trusses in the shape of a 2nd degree parabola, which in their opinion best corresponds to the actual shape of the structure. The value of the global imperfection amplitude was taken from [23] and [19], respectively, according to Section 5.3.3 (1). They used this model to obtain the interaction coefficients k_y, k_z (denoted k_{yy}, k_{yz}, k_{zy} a k_{zz} in Standard [19]). Subsequently, stability analyses were performed to determine the brace lengths of the individual rods.

We have the following comments on this part of the static recalculation:

a) The introduced shape of the initial buckling of the upper chord of the main beam corresponds to the buckling for the analysis of the stiffening systems and not for the chord itself. This is also supported by the very shapes of the stability loss of the truss structure. It is clear from the table on page 99 that the authors based the out-of-plane brace length of the chord on the order of twice the system length of the trusses (see also figure on page 100). It is not clear why a value derived from the second form of loss of out-of-plane stability was considered on page 94 and not from the first form of loss of out-of-plane stability of the main beam.

NOTE: With such a complex global analysis, the so-called Unified Global and Local Imperfection (UGLI) method according to 5.3.2 (11) in the Standard [19] could also be applied. Stability and non-linear analysis would have to be performed on a computational model with finer subdivision on the upper chord as well as on the infill rods of the main beam.

b) The intrinsic value of the imperfection amplitude given by the Standard [19] is the equivalent imperfection, which takes into account the influence of geometric and structural imperfections. In the case of riveted cross-sections, the influence of structural imperfections is significantly lower than in the case of welded cross-sections. The designers of the static recalculation could have taken into account the actual shape of the initial buckling of the pushed chord in the sense of Article A.2.1.15 in [25].

c) The procedure for determining the coefficients k_y and k_z by dividing the internal forces from GNIA by the internal forces from LA (linear analysis) can be accepted, but it does not correspond to the concept of the standard [19], in which these interaction coefficients also take into account the effect of the alternate bending moment.
Methodologically, then, these are no longer interaction coefficients, but just second-order theory influence factors. Since the global imperfections are already incorporated in the computational model for the global analysis, the capacity design should have been carried out on rods whose brace length is equal to the system length. The continuity of the structure is taken into account by the respective moments in the rod nodes (see Article 5.22(7b) in Standard [19]).

d) In the case of the analysis according to 6.3.3 (4) in Standard [19] with interaction coefficients k_{yy}, k_{yz}, k_{zy} a k_{zz}, a replacement rod with a length equal to the brace length is considered. The bending moments on the infill rods will be mostly trapezoidal or butterfly shaped. Thus, when considering a replacement rod with a brace length less than or not much greater than the theoretical length of the rod, these coefficients will result in coefficients less than 1.0. In the design presented in the static calculation, there is also another discrepancy with the Standard [19] in that the Standard relations 6.61 and 6.62 are used for the design of the resistance of rods, not sections, and the maximum internal forces on the rod are included.

Conclusion:

To account for the influence of second-order theory, the static recalculation authors applied a geometrically nonlinear analysis on the imperfect system. In our opinion, the imperfect system was not chosen appropriately. With such a complex global analysis as the recalculation compilers have performed, the Unified Global and Local Imperfection (UGLI) method according to 5.3.2 (11) in the Standard [19] could also be applied. When implementing the global imperfections in the global structural analysis, it is not necessary to verify the capacity of the surrogate rod (double-jointed), but the design is performed on a system-length rod. The interaction factors determined by the authors of the static recalculation, taking into account in this case only the influence of the second-order theory, reach relatively high values and are conservative for the infill rods. However, it is evident from the stability analysis that the influence of second-order theory is not significant for this construction.

4.2.7.2 Dynamic Analysis

The aim of the dynamic analysis was to obtain the actual vibration shapes of the structure and their corresponding frequencies, with the help of which the static recalculation processors verified in particular the stiffness assumptions introduced into the calculation model of the structure. At the same time, the theoretically obtained shapes and frequencies were confronted

with experimental measurements of these dynamic characteristics, which were carried out by the Faculty of Civil Engineering of the Czech Technical University in Prague under the direction of doc. Ing. Pavel Ryjáček, Ph.D. The results of the comparison of both approaches show good agreement and, except for a more significant deviation in the 2nd eigenmode, meet the criteria of permissible limiting deviation of frequencies.

Conclusion:

Our only comment on this analysis is that we lack the oscillation shape describing the 1st shape of the stability loss of the upper chord of the main beam. Usually, this shape also appears among the lowest frequencies of the bridge system oscillation.

4.2.7.3 Stress Range Spectra

The stress range spectra for the ultimate fatigue state assessment using the fatigue damage accumulation method for the period 2000 – 2055 were evaluated based on the dynamic analysis of the computational model (performed within the project [26]). The "Rainflow" sorting method was used to determine the stress spectra. These spectra were referenced to the relative spread from the C3 axle load category scheme. The number of relative spectrum cycles shows a huge increase in intensity from 2000 to 2055, especially in the period 2018–2022, which had a significant impact on the subsequent fatigue design and determination of the residual fatigue resistance of the structure.

The results of the dynamic analysis were confronted with the results of experimentally determined relative spectra of oscillations for the loads in both tracks related to the load level of the C3 axle load category. The comparison between experiment and numerical analysis can be characterised as satisfactory, which led the authors of the static recalculation to use the evaluated relative stress range spectra from the numerical analysis for the subsequent ultimate fatigue state assessment.

4.2.7.4 Analysis of the Interaction of the Rail-Track with the Main Beams

In this analysis, the flow of internal forces from the main beams to the bridge elements was monitored. The analysis mainly focused on:

- co-action of the rail-track – supporting cross bars,
- co-action of the rail-track – longitudinal trusses,
- taking into account the stiffness of the connection of the longitudinal trusses to the supporting cross bars,
- primary condition of the bridge at completion (without brake stiffeners),
- taking into account the primary condition of the bridge when it is completed (without reinforcement of the chords of the longitudinal trusses).

Based on the analysis of the behaviour of the calculation model of the rail-track section, the compilers of the static recalculation state that the behaviour of the calculation model corresponds to the functioning of the real structure and the set stiffnesses of the contact rods can be considered adequate.

Conclusion:

Our comments especially on the chosen stiffnesses of the rail-track element connections have already been presented in Section 4.2.6.

4.2.8 Determination of Load Capacity – Ultimate Limit States

Stresses at individual points were quantified in the cross-sections of the elements of the load-bearing structures, with subsequent relation to the design yield strength. The cross-sections have been assessed in the ultimate limit state assuming elastic action, i.e. as Class 3 cross-

sections in accordance with Article A. 2.2.4 v [25]. The total stress in the cross-sectional fibre under consideration was composed of partial stress components from individual groups of load conditions, which are linearly superposed.

The assessments were prepared in Excel spreadsheet and all have the same formal treatment. They are given in the annex to the static recalculation [5]. The relevant internal forces and cross-sectional characteristics used to determine the stresses from the relevant group of load cases are always indicated in the reports. The assessment is made for the most unfavourable combination of load groups for the critical edge fibres of the cross section (top, bottom and wall). The assessments are carried out in accordance with the Standards [19], [20], [23] and MP 2015 [25].

We have the following comments on this part of the static recalculation:

a) The elimination of duplication when considering corrosion weakening and rivet holes mentioned already on page 20 in [4] seems to be on the dangerous side in some cases. Examples are the lacing and perpendicular rod cuts in the transition to the lower chord panel point, where the rivet holes and deep local corrosion are very close together (figure on page 24 in [4], or figure on page 15 in Appendix [8]). Apparently, the load-bearing capacity of the cross-section should have been verified in an oblique section taking into account both the rivet hole and the missing part of the cross-section, or an assumption should have been introduced in the technical report for the structural recalculation that these details would be unconditionally corrected (see also comment in Section 4.2.2).

b) The designers of the conversion always multiply the specified load capacity Z_{LM71} by the effects from side impact and starting and braking forces. In cases where the load capacity is higher than 1.0, this is not correct, but leads to more conservative load capacities. Article 4.7.7 in MP 2015 [25] states that this procedure can be applied only in cases where the determined value of the load capacity $Z_{LM71} < 1.0$, while the other effects of the railway loading, i.e. the effects of lateral impact, starting and braking forces and centrifugal force, can be reduced in proportion to this determined load capacity.

c) By introducing a reduced bending stiffness of the infill rods of the main beams, the designers took into account the redistribution of internal forces within the global model. However, this does not mean that the effect of the interaction of global and local loss of stability of these rods can be neglected in the assessment. Thus, the brace of the partial rods between the couplings is not taken into account in the realised assessments. The statement in the note on page 91 is thus wrong. Thus, in our opinion, the design of the pushed infill rods is also incorrect and could lead to a reduction of the values of the specified load capacities for the split rods (see also comment in Section 4.2.6 of this assessment).

d) In the static recalculation, the verification of the load-bearing capacity of the connections and the determination of their load-bearing capacity is completely absent. This includes all connections, i.e. both truss rods and rail-track elements and their connections to the main beams. The load-bearing capacities of the neck rivets are also not verified.

   This is a fundamental comment. In fact, it was the riveted connections that showed the lowest load capacities in the static calculation of 2004 [24]. As an example, we present only 3 selected examples from the above recalculation:

   - connection of supporting cross bars to the main beam $Z_{UIC} = 0.41$,
   - connection of the longitudinal trusses to the supporting cross bar $Z_{UIC} = 0.65$,
   - connection of lacings to chords $Z_{UIC} = 0.73$.

The differences in load capacities compared to the 2004 assessment are thus essentially due to the failure to assess the riveted connections. These examples indicate that the specified load capacities in the static calculation are not the lowest possible. It is obvious that the connections can (and probably will) be a limiting element of the load carrying capacity of the bridge load-bearing structures in km 3.706 – Pod Vyšehradem, especially the connections of the rail-track elements.

Conclusion:

Of these comments, the one concerning the lack of assessment of all connections of the bridge load-bearing structure elements is very important. This is a serious deficiency that will significantly affect the conclusions of the static recalculation and the decision on the reconstruction of the entire bridge. It is necessary to analyse all connections of the bridge load-bearing structure elements and to assess the most stressed ones and determine their load capacity. Subsequently, the final conclusions of the static recalculation and the decision on the reconstruction method can be reconsidered.

4.2.9 Determination of Load Capacity – Ultimate Fatigue State

To assess the ultimate fatigue state and determine the residual fatigue life of the bridge load-bearing structures, the linear fatigue damage accumulation method according to the Palmgren-Miner hypothesis was used in accordance with the MP 2015 [25] and the Standard [22]. The assessment is carried out using stress range spectra determined from a very detailed survey of traffic loads on the bridge throughout the existing and planned future lifetime of the bridge after reconstruction.

The subject of the fatigue design are selected fatigue structural details, typical for riveted bridges, which are classified in accordance with the MP 2015 [25].

The established assumptions regarding the effect of two tracks on the bridge (percentage of trains meeting on the bridge), based on the evaluation of long-term monitoring of actual traffic on the bridge, are acceptable. Also the transformation of the standard stress range spectra according to ČSN 73 6203 to C3 axle load category together with the introduced corrections regarding the level of actual load effects for the global and local load carrying system seems to be correct.

In addition to the positive effect of the compressive stress range component on fatigue resistance (in the sense of MP 2015 [25] or the standard [22]), the negative effect of corrosion by reducing the fatigue strength is also taken into account, which was again based on the results of the aforementioned project [26].

The largely unfavourable results of the fatigue assessment are somewhat striking. Especially considering that the bridge has not had any serious problems with fatigue damage so far, which is also confirmed by the results of the detailed inspection of the steel load-bearing structures (Annex [8] of the project documentation), as well as the values of the calculated cumulative fatigue damage until 2018. A listing of the cumulative damage for the critical elements of the structure is given here, taken from the fatigue design recapitulation (Annex [5] of the static recalculation):

	1901–2018 (117 years)	2018–2055 (37 years)	1901–2055 (154 years)
- Diagonal D7 of the main beam:	0.622	0.329	0.951
- Supporting cross bar P3 – basic part:	0.513	1.371	1.884
- Longitudinal L2.E – centre:	0.666	2.111	2.777

Conclusion:

It is evident that the expected fatigue damage, especially of the bridge elements, is significantly (2.7 to 3.1 times) higher compared to the existing accumulated fatigue damage. It is debatable to what extent the enormously increased prospective effects of traffic loads (as determined in Chapter 2.5 of the static recalculation) are overestimated. Furthermore, given the values of the calculated cumulative fatigue damage for the period 2018–2055 (1.371 and 2.111 for the crossbeams and longitudinal trusses respectively), it is clear that simply replacing these elements will not ensure their required residual fatigue life to 2055, but that significant strengthening will be required to bring the above cumulative damage values below 1.0.

4.2.10 Ultimate Serviceability States

As part of the verification of the ultimate serviceability states, the transport safety criteria were verified in accordance with the requirements of the MP 2015 [25**]**.

Conclusion:

The load-bearing structure complies with the requirements of the MP 2015 [25] in terms of of ultimate serviceability states, except that exceeding the upper limit of the natural frequency limit is taken into account in the ultimate fatigue capacity assessment by means of a dynamic analysis for a characteristic train composition.

4.2.11 Assessment of Compatibility

Verification of the service load compatibility of TTZ C3/60 was performed for all sections and elements whose load capacity was $z_{LM71} < 1.0$ for a residual life of the load-bearing structures of 30 years. The compatibility of the load class was determined by direct calculation, i.e. the procedure according to Chapter 5 in MP 2015 [25**]** was not used**.** For the cross-sections of the elements that did not meet the compatibility criterion for the specified TTZ parameters and residual life, further verification was performed on the TTZ C3/60 for a residual life of 5 years. Since the elemental bridge deck cross bars did not meet this criterion, a re-verification of compatibility was performed for TTZ C3/40 for a residual life of 5 years, which the cross bars do meet. In addition, a compatibility assessment was carried out for the C2D2/40 hybrid TTZ assuming a residual life of 5 years, which the rail-track elements satisfied.

Conclusion:

The authors of the static recalculation state that the load-bearing structures of the bridge at 3.706 – Pod Vyšehradem are intermediate for TTZ C3/40 for a residual service life of 5 years. In connection with our comments regarding the non-verification of the load capacity of the riveted connections, it will be necessary to reassess these conclusions additionally, as the load capacity of the connections will probably be the limiting factor for determining the compatibility of the respective service load.

4.2.12 Conclusion of the Recalculation

The authors of the static recalculation state that the most accurate current procedures in the field of recalculations of railway bridge structures have been used to determine the load capacity and to assess the compatibility. In the assessment of cross-sections and elements, all the concessions given by the MP 2015 [25**]** were applied, taking into account the currently upcoming changes.

The results of the calculations were verified with experimentally determined values obtained in the verification static and dynamic test and with an independently developed calculation model for the dynamic analysis of the structure.

A summary overview of the static recalculation outputs is clearly presented in the table on p.
176 of the static recalculation [4], which shows that the bridge load-bearing structures are transient for TTZ C3/40 for a residual service life of 5 years.

Conclusion:

The final conclusions of the static recalculation of the bridge at km 3.706 – Pod Vyšehradem will have to be reassessed in connection with an additional assessment of the connections of all elements of the bridge's load-bearing structures.

4.2.13 Description of the Scope of Modifications

On the basis of the results of the static recalculation and verification of the compatibility of the operational load of TTZ C3/60 and TTZ C3/40, respectively, the authors propose reconstruction interventions in the form of replacement of non-compliant elements of the load-bearing structures in order to ensure the required compatibility of the operational load of TTZ C3/60 in the following range:

rail-track

- replacement and reinforcement of longitudinal trusses
- replacement and reinforcement of the crossbar chords, including change of the position of the end of the lamellas

main beams

- replacement of centre perpendiculars V. 4 to V. 8
- replacement of centre lacings D. 5 to D. 10

underbridge stiffening

- brake stiffener reinforcement
- reinforcement of the mullion of the stiffening over the rail-track.

Conclusion:

The list of reconstruction interventions will need to be expanded to include replacement or strengthening of the connections of the rail-track elements and their connections to the main beams, as well as the connections of the perpendiculars and lacings proposed for replacement. Also, when strengthening the brake stiffener and the mullion of the stiffening over the rail-track, it will be necessary to check their connections and, if necessary, propose their strengthening.

On the basis of additional verification of all connections in the bridge's load-bearing structures, reconstruction intervention is also possible at the connections of other elements.

4.3 Analysis of the Static Recalculation of the Substructure

4.3.1 General

The static recalculation was performed in category C in accordance with the MP 2015 [25**].** For the assessment of the ultimate limit states of the substructure, the combinations 6.10 according to the standard [14**]** were considered on the safe side for simplicity, the combinations 6.10a / 6.10b were not used. The partial load effect coefficients were considered for a substructure older than 30 years in accordance with the MP 2015 [25**].** For the design of the substructure, combinations of dominant loads from railway traffic and other non-dominant loads were considered, the values of combination coefficients are considered according to the Standard [14**]**. The static recalculation of the substructure also took into account the planned

repairs of the supports as part of the bridge reconstruction, so the load capacity is determined after reinforcement, not for their current condition.

In the expert assessment we focus only on our observations without extensive comments and descriptions.

4.3.2 Substructure – Piers

4.3.2.1 Material

The design strength of the masonry is determined assuming ideal intact masonry without cracks with a filling mortar of the prescribed composition. However, it is clear from the diagnostic survey that the masonry of the piers was found to be gapped and the masonry was diagnosed as moderately to coarsely porous. The calculation therefore assumes that this deficiency is removed (see 4.3.2.3 below).

4.3.2.2 Ultimate Limit State Assessment

The calculation of the load capacity is made only from the bearing capacity of the foundation joint under the caissons.

The resulting tensile stresses in the masonry are reduced by the proposed reinforcement using thin micropiles and therefore their effect on the actual load capacity is not evaluated.

The shear and shear strength of the masonry is not addressed at all. Apparently, this assessment is insignificant.

4.3.2.3 Conclusion

The specified load capacity of the piers is valid only after the masonry has been grouted and the tensile forces have been captured by the micropiles.

The design strength of the masonry is determined assuming the elimination of masonry imperfections, therefore it is stated in paragraph 2.3 that "*it is therefore recommended to grout the masonry of the substructure"*. The word "*recommended"* should therefore be replaced by the word ***"necessary"***.

4.3.3 Substructure – Abutment

4.3.3.1 Material

The design strength of the stone masonry of the abutment is determined assuming ideal intact masonry without cracks with a filling mortar of the prescribed composition. However, it is clear from the diagnostic survey that the abutment was also found to have gaps in the masonry. The calculation therefore assumes that this deficiency is removed (see 4.3.3.3 below).

4.3.3.2 Computational model

In the static recalculation, it is assumed that an ideal but also rigid load transfer from the timber piles to the load-bearing bedrock is ensured and the abutment is therefore further assessed as a surface-based heavy abutment. This assumption about the good condition of timber piles may be acceptable, but their pliability is probably significant. Therefore, we believe that accepting such an assumption is rather uncharitable. It is therefore necessary to consistently grout the abutment subsoil around the piles (see 4.3.3.4 below) or to assess the piles and consider abutment on a flexible subsoil.

4.3.3.3 Ultimate Limit State Assessment

The calculation of the load capacity is made only from the bearing capacity of the foundation joint. There is no quantification and assessment of possible tensile stresses in the masonry of the shank of the abutment.

It is assumed here that a layer of gravel and sand bedrock approximately 5–6 metres high will be reinforced by jet grouting (see 4.3.3.4 below).

4.3.3.4 Conclusion

The specified load capacity of the abutment is valid only after the masonry has been grouted and especially after the foundation joint subsoil layers have been grouted.

The design strength of the abutment masonry is determined, as with piers, assuming the elimination of masonry imperfections, therefore it is stated in paragraph 3.3 that "it is therefore recommended to grout the masonry of the substructure". The word "recommended" should therefore be replaced by the word **"necessary"**.

The same applies to the subsoil layers under the abutment (about 5–6 metres thick), as far as the assessment was carried out assuming sufficient bearing capacity but also stiffness. The conclusions then state that "*jet grouting of the area between the foundation joint and the R3 bedrock is recommended"*. Please note that the phrase "*is recommended"* should be replaced by "***is necessary"*** or the support should be recalculated using another more concise calculation model. However, the design of the grouting and its assessment in the recalculation is missing.

5. CONCLUSION OF THE EXPERT ASSESSMENT

The authors of the expert assessment state that the submitted static recalculation of the bridge at 3.706 – Pod Vyšehradem is prepared in accordance with the valid standards of ČSN EN and MP 2015 [25**]**. The recalculation of the bridge load-bearing structures was carried out in category D, the recalculation of the substructure in accordance with [25] in category C. Both recalculations, especially the recalculation of the load-bearing structures, are made to a high standard and with great care. The technical report for the static recalculation is very well prepared and complies with the requirements of [25**]**. It provided all the necessary information for the preparation of the expert assessment. Our detailed comments on the individual parts of the static recalculation are specified in the text of the expert assessment with a description of what, in our opinion, is missing or incorrect. Here we provide only a summary of what we believe to be the relevant deficiencies we have identified in the recalculation:

1. The results of the material tests were not statistically evaluated in the sense of Article 4.4.8 in [25], or statistical evaluation was not provided to the authors of this assessment. However, the conclusions drawn from the test results can be accepted.
2. It is not clear from the technical report for the structural recalculation which failures have been implemented in the calculation model of the bridge load-bearing structures and which have not been taken into account, as they are assumed to be removed by maintenance or repair as required by Article 4.1.2 in [25].
3. The considered wind load on the windward beam of 100% and on the outermost beam only 50% is contrary to the Standard [16], but it can be accepted. However, this reduced wind load on the outermost beam should have been applied only up to the amount of the traffic load. Thus, from a height of 4.0 m from the top of the rails it is necessary to load both main beams with the full wind load.
4. The estimate of the prospective traffic load appears to be significantly overestimated and significantly reduces the fatigue life of the bridge load-bearing structures.
5. The introduction of semi-rigid panel points and connections can be welcomed. However, it is questionable whether the stiffnesses of the nodes determined on the submodels give reliable information about their actual action in the structure. In our opinion, the stiffnesses of the connections of the rail-track elements and their connections to the main beams are underestimated.
6. We consider the reduction of the bending stiffnesses of the segmented rods to their immaterial axes in the computational model of the whole structure to be insignificantly high. This approach leads to an overestimation of the influence of the shear compliance of

the rod, on the other hand it does not take into account the interaction of the global and local brace of the rod.

7. The imperfect system for the nonlinear calculation was not chosen appropriately. The introduced shape of the initial buckling of the upper chord of the main beam corresponds to the buckling for the analysis of the stiffening systems and not for the analysis of the chord itself. In our opinion, the shape of the initial buckling should have been based on stability analysis. In this context, the so-called Unified Global and Local Imperfection (UGLI) method according to 5.3.2 (11) in standard [19] could be used. However, the influence of second-order theory is not significant.
8. Since the global imperfections were incorporated into the calculation model for the global analysis, the capacity design should have been carried out on rods whose brace length is equal to the system length according to Article 5.22(7b) in the Standard [19]).
9. The interaction factors determined by the authors of the static recalculation, taking into account in this case only the influence of the second-order theory, reach relatively high values and are conservative for the infill rods.
10. The influence of the interaction of the global and local loss of stability of these rods was not taken into account in the assessments of the segmented rods, since the brace of the sub-rods between the connectors is not included in the assessments carried out.
11. In the static recalculation, the verification of the load-bearing capacity of the connections and the determination of their load-bearing capacity is completely absent. This includes all connections, i.e. both truss rods and rail-track elements and their connections to the main beams. The load-bearing capacities of the neck rivets are also not verified. This is a serious deficiency that will significantly affect the conclusions of the static recalculation and the decision on the reconstruction of the entire bridge.
12. It is debatable to what extent the enormously increased prospective effects of traffic loads are overestimated. Furthermore, given the values of the calculated cumulative fatigue damage for the period 2018–2055 (1.371 and 2.111 for the crossbeams and longitudinal trusses respectively), it is clear that simply replacing these elements will not ensure their required residual fatigue life to 2055, but that significant strengthening will be required to bring the above cumulative damage values below 1.0.
13. The list of reconstruction interventions will need to be expanded to include replacement or strengthening of the connections of the rail-track elements and their connections to the main beams, as well as the connections of the perpendiculars and lacings proposed for replacement. Also, when strengthening the brake stiffener and the mullion of the stiffening over the rail-track, it will be necessary to check their connections and, if necessary, propose their strengthening. On the basis of additional verification of all connections in the bridge's load-bearing structures, reconstruction intervention is also possible at the connections of other elements.
14. The specified load capacity of the piers is valid only after the masonry has been grouted and the tensile forces have been captured by the micropiles.
15. The specified load capacity of the abutment is valid only after the masonry has been grouted and especially after the foundation joint subsoil layers have been grouted.

Žilina, dated 20/08/2018

Prepared by: prof. Ing. Josef Vičan, CSc.

Ing. Jaroslav Odrobiňák, PhD.

Ing. Jozef Gocál, PhD.